Detection of Distributed Deterioration in Single Pipes Using Transient Reflections

Jinzhe Gong[1], Angus R. Simpson[2], Martin F. Lambert[3], Aaron C. Zecchin[4], Young-il Kim[5], and Arris S. Tijsseling[6]

[1]PhD Candidate; School of Civil, Environmental and Mining Engineering, University of Adelaide, SA 5005, Australia; Email: jinzhe.gong@adelaide.edu.au

[2]Professor; School of Civil, Environmental and Mining Engineering, University of Adelaide, SA 5005, Australia; Email: angus.simpson@adelaide.edu.au

[3]Professor; School of Civil, Environmental and Mining Engineering, University of Adelaide, SA 5005, Australia; Email: martin.lambert@adelaide.edu.au

[4]Lecturer; School of Civil, Environmental and Mining Engineering, University of Adelaide, SA 5005, Australia; Email: aaron.zecchin@adelaide.edu.au

[5]Research Associate; School of Civil, Environmental and Mining Engineering, University of Adelaide, SA 5005, Australia; Email: youngil.kim@adelaide.edu.au

[6]Assistant Professor; Department of Mathematics and Computer Science, Eindhoven University of Technology, The Netherlands; Email: a.s.tijsseling@tue.nl

ABSTRACT

A number of different methods that use signal processing of fluid transients (water hammer waves) for fault detection in pipes have been proposed in the last two decades. However, most of them focus solely on the detection of discrete deterioration, such as

leaks or discrete blockages. Few studies have been conducted on the detection of distributed deterioration, such as extended sections of corrosion and extended blockages. This is despite the fact that they commonly exist and can have a severe negative impact on the operation of pipelines. The research reported here proposes a method of detecting distributed deterioration by investigating the time-domain water hammer response trace from a single pipe with a deteriorated section. Through wave analysis using a step pressure input, a theoretical square-shaped perturbation is found to exist in the transient pressure trace as a result of distributed deterioration. The hydraulic impedance of this section can be derived from the magnitude of the reflected pressure perturbation, while the location and length of the corresponding deteriorated section can be determined by using the arrival time and duration of the perturbation. The proposed method has been validated by analyzing experimental data measured from a pipe with a section of wall thickness change.

INTRODUCTION

In the last two decades, a number of transient-based fault detection methods have been developed for water transmission pipelines (Colombo et al. 2009). Transient-based methods are promising and attractive because they are non-invasive, simple to perform and can provide information about a lengthy section of pipe (hundreds to thousands of meters). While most transient-based fault detection methods focus on the detection of discrete elements, such as leaks (Wang et al. 2002; Lee et al. 2005; Lee et al. 2007a) and

discrete (partial) blockages (Vítkovský et al. 2003; Lee et al. 2008), the detection of distributed elements has not attracted much attention. However, distributed deterioration, such as extended corrosion or blockages (Arbon et al. 2007), cement mortar lining spalling (Stephens et al. 2008), and pipeline sections with a lower pressure rating (mistakenly installed), sometimes exist in real pipelines and impose negative impacts on the operation of fluid transmission. According to a previous field study in South Australia (Stephens et al. 2008), sections with significant cement mortar lining spalling and internal corrosion, typically with a length around 10 meters each, were observed intermittently along the water transmission pipeline that was tested. Distributed deterioration can reduce water transmission efficiency (Tran et al. 2010), create water quality problems (Vreeburg and Boxall 2007), and critically, may also develop into bursts or severe blockages over time (Zamanzadeh et al. 2007). Techniques for the non-invasive detection of distributed deterioration are required.

The current paper presents a transient-based distributed deterioration detection method for single water transmission pipelines based on time-domain reflectometry (TDR) (Lee et al. 2007b). An incident wave is assumed to propagate along a pipeline that has a section of distributed deterioration, in which the hydraulic impedance is different from the impedance of other parts of the pipeline. The pressure transient trace of this pipeline is measured at the point of generation of the incident wave. The process of the wave propagating through the deteriorated section is analyzed using the method of characteristics (MOC) (Wylie and Streeter 1993). The analysis illustrates that the

properties of the distributed deterioration can be determined from the theoretical square-shaped perturbation in the measured pressure trace. Experimental verification of the proposed distributed deterioration detection method is performed by analyzing the data gathered from a pipeline with a section exhibiting changes in wall thickness. The impedance, wall thickness, wave speed, location and length of this section are successfully estimated.

BACKGROUND

The physical foundation of the proposed TDR-based distributed deterioration detection method is presented here. A distributed deterioration in a single pipeline introduces an extended hydraulic impedance change. Reflections occur when a transient wave comes across impedance discontinuities, which are the boundaries of the distributed deterioration. The reflected signals are dependent on the location, length and hydraulic impedance of the deteriorated section, and so are indicators of the deterioration.

The characteristic impedance B of a uniform pipeline is defined as

$$B = a / (gA) \tag{1}$$

where a is the wave speed of the transient wave; A is the internal cross-sectional area of the pipeline; and g is the gravitational acceleration. The impedance is sensitive to the pipeline wall thickness. A change in wall thickness affects not only the internal cross-

sectional area but it also affects the wave speed, where the wave speed and wall thickness are related by the wave speed formula (Wylie and Streeter 1993):

$$a = \sqrt{\frac{K/\rho}{1+(K/E)(D/e)c_1}} \tag{2}$$

in which, K is the bulk modulus of the transmitted fluid; ρ is the density of the fluid; E is Young's modulus of the wall material; D is the internal diameter of the pipeline; e is the wall thickness; c_1 is an uncertain factor close to 1, depending on the structural restraint condition of the pipeline (Wylie and Streeter 1993).

The chemical and physical mechanisms of material deterioration, such as corrosion, tuberculation and graphitization, in water distribution pipelines are complex (Rajani and Kleiner 2001; Sarin et al. 2001; Nawrocki et al. 2010). However, when a section of extended corrosion or blockage is present, generally the wall thickness is changed. Young's modulus may also alter due to changes in the pipe wall material. All of these factors may lead to a change in the hydraulic impedance of the pipeline according to Eqs (1) and (2). For example, assuming that the bulk modulus of water and Young's modulus of the pipe wall remain constant, then according to Eq. (2), a thinner wall thickness due to internal corrosion results in a slightly larger internal diameter and a smaller wave speed, thereby yielding a smaller value of characteristic impedance. Similarly, a higher impedance value is expected if the wall becomes thicker.

In real pipes, the distribution and pattern of deterioration can be complex. For simplicity, this paper only considers uniformly distributed deterioration, i.e. sections with uniform anomalous impedance existing in a single pipeline.

WAVE PROPAGATION ANALYSIS

The behavior of a transient wave propagating without attenuation through a deteriorated section with a lower impedance value is analyzed using the MOC. The process of wave reflection and transmission at the boundaries of the deteriorated section is illustrated in Fig. 1. The two vertical solid lines in the pipeline stand for the two boundaries (interfaces) of the deterioration. The hydraulic impedance of the deteriorated section is B_1 and the impedance of the original pipeline is B_0. Four wave propagating stages, and corresponding hydraulic grade lines (HGLs), at different time stages are displayed.

In Fig. 1(a), the steady-state head is H_0 and the steady-state flow rate is Q_0, discharging from left to right. An incident wave W_0 with a magnitude of H_i is approaching the first interface (the right boundary) from the right side. In Fig. 1(b), the first reflection occurred at the first interface. Part of the wave is reflected as W_{r1} and the remainder is transmitted as W_{t1}. Based on the MOC analysis of pipelines in series performed by Wylie (1983), three compatibility equations can be used to describe the wave reflection and transmission at the right boundary:

$$H_{j1} = H_0 + B_1 Q_0 - B_1 Q_{j1} \tag{3}$$

$$H_{j1} = H_i - B_0 Q_i + B_0 Q_{j1} \tag{4}$$

$$H_i = H_0 + B_0 Q_0 - B_0 Q_i \tag{5}$$

where H_{j1} and Q_{j1} are the head and flow after the first reflection and transmission. Solving the above equations for H_{j1} and Q_{j1} yields:

$$H_{j1} = H_0 + \frac{2B_1}{B_0 + B_1}(H_i - H_0) \tag{6}$$

$$Q_{j1} = Q_0 + \frac{2B_0}{B_0 + B_1}(Q_i - Q_0) \tag{7}$$

Eq. (6) illustrates the fact that the value of the head after the first reflection, H_{j1}, is dependent on the values of B_0 and B_1. Provided the deterioration has a lower impedance value than the original pipe (i.e. $B_1 < B_0$), the value of H_{j1} will be smaller than the value of the original incident wave head H_i. A step drop will occur in the HGL. The transmitted wave W_{t1} will be reflected again at the second boundary (left boundary) of the deteriorated section [see Fig. 1(c)]. When W_{t1} is propagating from the low impedance section to the high impedance section, the value of the head after reflection and transmission, H_{j2}, will be higher than H_{j1}. Similarly, when the second reflected wave, W_{r2}, comes across the first boundary, the head will increase again [see Fig. 1(d)]. A step rise will be observed in the HGL.

After the three steps, a head perturbation with a square shape will propagate along the pipeline. The head value of the perturbation wave is H_{j1} and the wave duration is the time required by the transient wave to travel twice the length of the deteriorated section

$$T_1 = 2L_1 / a_1 \tag{8}$$

where L_1 is the length of the anomalous deteriorated section and a_1 is the wave speed along this section. If the incident wave started from the measurement station (the location of the transducer) at time zero, the arrival time of the head perturbation is:

$$T_0 = 2L_0 / a_0 \tag{9}$$

where L_0 is the length between the transducer and the first encountered boundary of the deteriorated pipe section; and a_0 is the wave speed in the original intact pipeline.

DISTRIBUTED DETERIORATION DETECTION PROCEDURES

Two distributed deterioration detection procedures with different detection configurations can be developed based on the previous wave propagation analysis. One procedure is used for detecting deterioration based on a transient generator and a pressure transducer located at a closed end of a pipeline; another procedure is used when the transient wave is generated and the pressure response is measured at any interior location along the pipe.

Detection at the end of a pipeline

For a reservoir-pipeline-valve system, an incident wave can be generated by a fast valve closure. A point just upstream from the valve is the best position for pressure wave observation, because the incident wave starts from this point and reflected signals will be reinforced at the closed valve (Lee et al. 2006). The head value of the incident (H_i) caused by the valve closure can be calculated using either the Joukowsky head change equation (Wylie and Streeter 1993) or MOC analysis, and is written as

$$H_i = H_0 + B_0 Q_0 \tag{10}$$

The flow rate Q_i is zero after the valve is fully closed. Substituting Q_i = 0 into Eq. (7) yields the following expression for Q_{j1}:

$$Q_{j1} = \frac{B_1 - B_0}{B_0 + B_1} Q_0 \tag{11}$$

When the reflected wave W_{r1} [see Fig. 1(d)] arrives at the end of the pipeline, where the transducer is located, the flow remains zero. Using the Joukowsky head change equation, the observed head of the reflection is:

$$H_p = H_{j1} + B_0 Q_{j1} \tag{12}$$

Substituting Eqs (6) and (11) into Eq. (12), and using $H_i - H_0$ to replace $B_0 Q_0$, H_p can be rewritten as

$$H_p = H_0 + \frac{3B_1 - B_0}{B_1 + B_0}(H_i - H_0) \tag{13}$$

This head level will last until the wave front W_{t3} [see Fig. 1(d)] arrives at the transducer, which makes the completion of the theoretical square-shaped perturbation.

The impedance difference between the deteriorated section and the original pipeline is defined as $\Delta B = B_1 - B_0$. Substituting ΔB into Eq. (13) and rearranging it, the equation can be presented as

$$\frac{\Delta B}{B_0 + \Delta B/2} = \frac{\Delta H}{\tilde{H}_i} \tag{14}$$

where $\Delta H = H_p - H_i$ is the magnitude of the deterioration-induced head perturbation; and $\tilde{H}_i = H_i - H_0 = B_0 Q_0$ is the magnitude of the incident wave, i.e. the head rise caused by the incident wave. Eq. (14) indicates that the impedance difference ΔB is only related to the impedance of the original pipeline B_0 and the magnitude ratio of the reflected disturbance to the incident wave $\Delta H / \tilde{H}_i$. The value of B_0 can be determined from Eq. (1) and the value of $\Delta H / \tilde{H}_i$ can be estimated from the measured pressure trace. Eq. (14) also illustrates that the ratio $\Delta H / \tilde{H}_i$ is independent of the steady-state head H_0 and flow rate Q_0, so that theoretically the impedance difference ΔB can be determined with arbitrary steady-state condition, provided the ratio can be accurately estimated from the measured pressure trace. Rearranging Eq. (14), finally the expression for ΔB is

$$\Delta B = \frac{2B_0 \, \Delta H / \tilde{H}_i}{2 - \Delta H / \tilde{H}_i} \tag{15}$$

If the change in impedance is caused only by a uniform wall thickness change, and the external diameter of the deteriorated section is known, the wall thickness and wave speed in this section can be determined using the definition of the pipeline impedance [Eq. (1)] and the wave speed formula [Eq. (2)]. The location and length of the deteriorated section can then be determined using Eqs. (8) and (9).

The above analysis applies only to wave reflections resulting from the deterioration within the first $2L/a$ of the transient trace (the first plateau), where L is the total length of the pipeline and a is the representative wave speed for the whole pipeline. Due to the effect of multiple reflections between the pipeline terminals and the boundaries of the deterioration, complex disturbances are expected in the pressure trace after the time of $2L/a$.

Detection at an interior location

A major advantage of generating the transient wave and measuring the pressure at an interior location is that the fluid transmission continues during the whole detection procedure, i.e. a base flow rate is maintained and only slight flow perturbations are imposed. A side-discharge valve and a transducer can be placed at any location along the pipeline. They can be situated at the same point or at different points. Fig. 2 illustrates the layout of the detection system.

Assume the steady-state head at the side-discharge valve is H_0, the flow through the valve is Q_v, and the flow rates at the upstream side and the downstream side of the valve are Q_1 and Q_2 respectively [Fig. 2(a)]. A fast closure of the side-discharge valve leads to two symmetric incident waves propagating along two opposite directions in the main pipeline [Fig. 2(b)]. The head and flow of the incident waves can be derived as:

$$H_i = H_0 + B_0 Q_v / 2 \tag{16}$$

$$Q_i = (Q_1 + Q_2)/2 \tag{17}$$

If a deteriorated section is located at the upstream side of the side-discharge valve, reflections will occur at the boundaries of the deteriorated section. The whole procedure is the same as that shown in Fig. 1. The head and flow for the reflected perturbation are:

$$H_p = H_0 + \frac{B_0 B_1}{B_0 + B_1} Q_v \tag{18}$$

$$Q_p = \frac{B_1 Q_1 + B_0 Q_2}{B_0 + B_1} \tag{19}$$

A transducer located at the downstream side of the deteriorated section can measure the reflected head perturbation H_p. The value of H_p can be used to determine the impedance of the deteriorated section. The location and length of the deteriorated section can be derived using the arrival time and duration of this head perturbation signal, provided the locations of the transducer and side-discharge valve are known.

In real applications, the relative location of the deteriorated section is unknown and generally three possible situations exist: The deteriorated section can be either between the transient generator and the transducer or at one side (upstream or downstream) of the two. Multiple solutions to the location of the deterioration can be obtained from a single time-domain transient trace. Lee et al. (2007b) analyzed this practical issue for leak detection and provided techniques to determine the origin of the reflection. However, more complex situations can be encountered in distributed deterioration detection. For example, the generator and/or the transducer may also be accidentally positioned within the deteriorated zone, and multiple deteriorated sections may introduce complex pressure responses.

DISTRIBUTED VERSUS DISCRETE DETERIORATION

In real world pipelines, both distributed (such as corrosion and extended blockages) and discrete deterioration (such as leaks and discrete blockages) may exist. The different types of deterioration can be determined from the measured transient pressure traces.

When a step wave is used as the excitation, a leak can introduce a pressure drop in the measured pressure trace (Lee et al. 2007a), while the reflection from a discrete blockage shows as a pressure jump (Kim et al. 2007). In contrast, a distributed deterioration introduces a square-shaped reflection. The square is either negative (lower than the head of the incident wave) for a deteriorated section with a lower impedance, or positive

(higher than the head of the incident wave) when it has a higher impedance than the original pipeline. However, if both a leak and a discrete blockage exist in a single pipeline, the pattern of reflection could be similar to the square-shaped disturbance resulting from a distributed deterioration. In order to determine the type of the deterioration, the transient generation and pressure measurement needs to be performed on both the upstream and the downstream sides of the deterioration. For a distributed deterioration, the pattern of the square-shaped reflection is constant. For example, if the deterioration is a pipe section with a lower impedance, the reflection always has a negative square shape, no matter the transient generation and pressure measurement is taken at the upstream or the downstream side. In contrast, the two square-shaped reflections resulting from two local discontinuities will show opposite patterns, i.e. one is positive and the other is negative.

EXPERIMENTAL VERIFICATION

System configuration

Laboratory experiments were conducted to validate the proposed distributed deterioration detection method. The test pipeline was a 37.46 m straight copper pipe with an external diameter of 25.4 mm, an internal diameter D_0 = 22.14 mm, and a wall thickness e_0 = 1.63 mm. One end of the pipeline was connected to an electronically controlled pressurized tank and the other end was a closed in-line valve. The pipeline was fixed rigidly to a support structure on the wall to prevent vibration during transient

events. A pipe section 1.649 m long with a thinner pipe wall thickness was placed 17.805 m upstream from the in-line valve. While the material and external diameter of this section were the same as those of the original pipeline, the internal diameter D_1 = 22.96 mm and the wall thickness e_1 = 1.22 mm. This section represents a pipe section with a lower pressure rating, or a section with uniform wall thickness that has decreased due to internal corrosion, neglecting the effects of spatial variability as would be present in realistic corroded sections.

A transient wave was generated by sharply closing a side-discharge solenoid valve 144 mm upstream from the closed in-line valve (the closure time was approximately 4 ms). Pressure responses were monitored at the side-discharge valve with a sampling rate of 2 kHz. The pressure transducer was a Druck PDCR 810 high integrity silicon flush mounted diaphragm transducer with an absolute pressure range of 0 to 15 bar. The rise time of the transducer was estimated to be 5 micro seconds (Lee et al. 2007b). A customized amplifier with carefully designed adjustable filtering and adjustable pressure ranges was used and the response frequency was 16 kHz. The pipeline system layout is illustrated in Fig. 3.

Experimental pressure traces

Fig. 4 gives an overview of the pressure transient trace as measured from Test 1. The transient response trace has a periodic pattern due to reflections at two pipeline ends.

Signal attenuation, dissipation and dispersion can also be observed, but the influence of friction is negligible for the first plateau. In addition to the pressure perturbation that appears in the middle of the first plateau (of duration $2L/a$), complex perturbations due to multi-reflections are present in the following time.

To verify the repeatability of the experiments, a number of tests have been conducted with the same pipeline configuration. Experiments on an intact pipeline were also performed for comparison. The first plateau (of duration $2L/a$) of the measured pressure traces for three tests on a pipeline with a thinner wall section (Tests 1 to 3) and of one test on an intact pipeline (marked as 'Intact') are shown in Fig. 5. The pressure traces of Tests 1 to 3 are similar, with a pressure perturbation located at the middle of the plateau. The response from an intact pipe shows a nearly flat pattern, as is expected.

Determination of the impedance, wave speed and wall thickness

Fig. 6 gives an enlarged view of the pressure rise during valve closure measured in Test 1, and Fig. 7 shows an enlarged view of the pressure perturbation in the first plateau of the pressure trace in Test 1. A pressure drop followed by a pressure rise (Fig. 7) indicates that the reflection comes from a section with lower impedance. The reflected perturbation does not show a clear square shape as seen in the theoretical analysis (Fig. 1), mainly because the wave front of the incident wave due to valve closure (Fig. 6) is not a true vertical step, but rather it is a curve that has a total rise time T_r of around 4 ms

(from 6.941 s to 6.945 s). The influence of the shape and rise time of the initial wave front will be discussed later in the paper.

The wave speed (a_0) in the intact pipeline was 1328 m/s as determined by experiments (Lee et al. 2007b; Kim 2008). Using Eq. (1), the impedance of the original pipeline (B_0) is 3.516×10^5 s/m^2. The parameter c_1 in the wave speed formula [Eq. (2)] is estimated as 1.006 using the theoretical equation for thick-walled elastic pipeline provided in Wylie and Streeter (1993). The steady-state head is estimated to be H_0 = 25.55 m by averaging the pressure values within a short time interval before the wave front (6.92 s to 6.94 s). Similarly, the head value of the incident wave can be estimated from the first plateau and it is H_i = 39.06 m (by averaging the pressure from 6.945 s to 6.947 s). As a result, the magnitude of the incident wave is $\tilde{H}_i = H_i - H_0$ = 13.51 m. The lowest head value in the reflected pressure disturbance shown in Fig. 7 is H_p = 37.86 m, so that the magnitude of the disturbance is $\Delta H = H_p - H_i$ = –1.20 m. Finally, by using Eq. (15), the impedance difference between the deterioration and the original pipeline is estimated as ΔB = –29, 900 s/m^2. The impedance of the deterioration is determined to be B_1 = 3.217×10^5 s/m^2.

The deterioration is known to be a section with a uniform wall thickness change. Knowing B_1 and using the definition of impedance [Eq. (1)] and the wave speed formula

[Eq. (2)], the wave speed and wall thickness of the deteriorated section are estimated as a_1 = 1292 m/s and e_1 = 1.29 mm, respectively. In this research, the *Goal Seek* function in Microsoft Excel is used to solve these equations.

The pressure traces in Tests 2 and 3 are also interpreted. Finally, the impedance B_1, wave speed a_1 and wall thickness e_1 of the deterioration that have been estimated from the three laboratory experiments are listed in Table 1. The analytical values of B_1, a_1 and e_1 for the actual wall thickness e_1 = 1.22 mm are also calculated and listed in the first row as the bench marks. The relative errors for the experimental results are calculated. The 'relative error' is defined as '|(value estimated from tests – analytical value) / analytical value|$\times$100%'.

It can be seen from Table 1 that the estimated properties of the deteriorated section are close to the analytical results. It verifies that the distributed determination can be detected and its properties can be estimated from the water hammer pressure trace using the proposed technique. However, the relative errors in B_1, a_1 and e_1 are always small because their theoretical values are large compared with the absolute difference between the deterioration and the original pipeline. For example, the theoretical value of B_1 is approximately 10 times of the theoretical impedance difference between the deterioration and the original pipeline. The accuracy of the proposed technique can be

further studied from the estimated impedance difference ΔB, wave speed difference Δa and wall thickness difference Δe.

The experimental results of the impedance difference ΔB, the wave speed difference Δa and the wall thickness difference Δe are compared with the analytical values for the actual B_1, a_1 and e_1 = 1.22 mm, as shown in Table 2. Relative errors are calculated using the same definition as used in Table 1.

It can be seen from Table 2 that ΔB, Δa and Δe all have a relative error of about 20 %. The error is acceptable, but it is much higher than the error shown in Table 1. In addition to the uncertainties in the laboratory pipeline, one source of error may come from the experimental wave front. Due to the limitation in the maneuverability of the valve, the initial wave front of the transient waves used in the experiments is curved rather than a theoretical vertical step. To study the effect of the initial wave front, numerical simulations are performed as described below.

The influence of the initial wave front

As mentioned in the previous section, the initial wave front in Test 1 (Fig. 6) is a 4 ms curve rather than a true vertical step. This is inevitable due to limitation in the maneuverability of real world valves. The curved wave front is assumed to be the major

reason for the distortion in the reflected pressure disturbance, making it a smooth dip rather than a sharp square shape.

According to the wave propagation analysis shown in Fig. 1, the interval between the first reflection and transmission [Fig. 1(b)] and the third reflection and transmission [Fig. 1 (d)] is $2L_1 / a_1$, where L_1 = length of deteriorated section with impedance B_1 and wave speed a_1. If the rise time of the incident wave T_r is more than $2L_1 / a_1$, the wave W_{r2} (which is reflected from the left boundary of the deterioration), will overlap with the original incident wave W_0 at the right boundary. As a result, the theoretical spatial resolution (the theoretical shortest deterioration length that can be accurately detected) is $T_r a_1 / 2$.

The estimated value of $2L_1 / a_1$ is 2.6 ms for the experimental pipeline. It is smaller than the duration of the wave front T_r (4 ms), implying that wave overlapping did occur and the resulting impedance determined using Eq. (15) is compromised. However, it can be seen from Fig. 6 that, although the whole wave front lasts 4 ms, the major pressure rise occurs within only 2.5 ms which is just less than $2L_1 / a_1$. As shown in Fig. 6, the major pressure change occurred between 6.942 s and 6.9445 s. The pressure increased from 25.94 m to 39.00 m during the 2.5 ms, which is 97 % of the total pressure rise. As a

result, it is expected that the experimental initial wave front will not have much influence on the accuracy in the estimation of ΔB, Δa and Δe.

To study in detail the influence of the initial wave front, numerical water hammer simulations have been conducted. The pipeline configuration used in the numerical simulations was the same as the experimental configuration as illustrated in Fig. 3, except that the side-discharge valve was removed and the transient wave was generated by the in-line valve at the end. The method of characteristics (MOC) was used to perform the numerical modeling and the resolution was 0.01 ms. Friction is neglected in the numerical simulations, because the influence of friction is negligible for the first plateau of the transient trace.

Three different cases were considered: Case 1, a vertical wave front (starting at 6.945 s, which is the time point of the full valve closure in Test 1) was adopted to determine the theoretical pressure response; Case 2, the measured wave front shown in Fig. 6 was interpolated and used as the input in the MOC modeling; and Case 3, a third study has been performed on a modified pipeline configuration, in which the input was the measured pressure curve, but the length of the deteriorated section was doubled to 3.30 m to make $2L_1 / a_1$ (5.2 ms) longer than T_r (4 ms).

For these three case studies, the steady-state head (H_0) and the head of the incident wave (H_i) are all the same, so that the magnitudes of the incident wave are uniform ($\tilde{H}_i$ = 13.51 m). Three pressure traces were obtained numerically, one for each case, as shown in Fig. 8. The pressure trace measured in the experimental Test 1 is also presented for comparison. The enlargement of the deterioration-induced pressure perturbations are shown in Fig. 9.

To study the effect of the initial wave front on the accuracy of the estimated impedance difference ΔB, firstly the magnitude of the deterioration-induced perturbation ΔH is estimated for each case study from its numerical pressure trace. For Cases 2 and 3 with the curved initial wave front, the magnitude of the perturbation is defined as the head difference between the lowest pressure point in the perturbation and the head of the incident wave. Table 3 summarizes the values of ΔH for the three numerical case studies, and the corresponding estimated impedance difference ΔB. Analytical values are presented in the first row as bench marks, which are calculated for the theoretical impedance of the deteriorated section $B_1 = 3.151\times10^5$ s/m^2 using Eq. (14) and the magnitude of the incident wave $\tilde{H}_i = 13.51$ m. The relative deviation from the analytical value is calculated for each numerically determined ΔH, which is defined as '|(value estimated from numerical simulations – analytical value) / analytical value|$\times$100 %'.

It can be seen from Table 3 that the results derived from the numerical pressure trace in Case 1 (vertical wave front) are exactly the same as the analytical results, as is expected. This case study indicates that the impedance of the deterioration can be determined accurately when the incident wave has a vertical wave front. The numerical pressure trace of Case 1 can be used as the bench mark in Fig. 9.

The deterioration-induced perturbation obtained numerically in Case 2 (measured wave front) is consistent with the experimental pressure perturbation in Test 1 (laboratory experiment) in shape and time, as is expected. However, the magnitude of the disturbance ΔH in Case 2 is only 2.7 % smaller than the analytical value. The impedance difference ΔB estimated in Case 2 also shows a high accuracy. These results verify the previous assumption that, although the curved experimental wave front has a total rise time (4 ms) that is greater than $2L_1 / a_1$, the effects of the wave overlapping is small because the major pressure rise (more than 97 % of the total head rise) occurs within a time interval less than $2L_1 / a_1$.

The result from Case 3 (double length deterioration) shows that when $2L_1 / a_1$ is longer than the rise time T_r, the reflected pressure disturbance does reach the theoretical straight bottom line (Case 1) and lasts for a short period of time before increasing again. From additional numerical testing, the duration is observed to be $2L_1 / a_1 - T_r$.

The magnitude of the reflected disturbance estimated in the laboratory experiment Test 1 is ΔH = –1.20 m, which has a relative error of 16.7 % compared with the theoretical value for Case 2 (–1.44 m). The error in the estimated ΔH leads to errors in the estimated ΔB, Δa and Δe, as depicted in Table 2. To these errors, the contribution from the curved wave front is small, as discussed previously in the numerical study of Case 2. Other sources of experimental error includes the effects from the small hydraulic components in the pipeline (such as joints and the customized brass block that is used to install the pressure transducer and the side-discharge valve), the micro-perturbations that are always shown in the experimental pressure traces (even in the steady state), and the compromise in data due to sampling. It is expected that increasing the magnitude of the incident wave can increase the accuracy in the estimation assuming that the noise level remains the same, because the magnitude of the reflected disturbance is proportional to the magnitude of the incident wave.

Determination of the location and length

To estimate the location and length of the deteriorated section, the arrival time (T_0) and duration (T_1) of the reflected disturbance need to be estimated. From Fig. 6 and Fig. 7, the time between the end point of the wave front (6.945 s) and the lowest value in the reflected head disturbance (6.9715 s) is 0.0265 s. Then this value is used as T_0 in Eq. (9), and the deteriorated section is estimated to be 17.60 m upstream from the in-line valve.

The time T_1 in Eq. (8) is hard to estimate from the experimental pressure trace. From the numerical simulations shown in Fig. 9, the duration of the deterioration-induced pressure dip can be the time interval between the start of the dip and the end of the straight bottom if $2L_1 / a_1$ is greater than T_r (this is Case 3 in Fig. 9). The time from when the dip starts can be estimated from the first pressure datum in the experimental pressure disturbance that is lower than the head of the incident wave (H_i). From Fig. 7 and using $H_i = 39.06$ m as a threshold, the starting time of the dip is 6.9675 s. However, the measured pressure dip shows a sharp tip at the bottom (at 6.9715 s in Fig. 9) rather than a theoretical straight line, which suggests that $2L_1 / a_1$ is smaller than T_r in the experiment. If no prior information is known, this lowest point has to be used as the end point. As a result, the value of T_1 is estimated to be 0.0040 s. Using Eq. (8) and the estimated wave speed in the deterioration as shown in Table 1, the length of the pipe section with the thinner wall is estimated as 2.56 m, which is much larger than the actual value of 1.649 m. The experimental results of the location and length of the deterioration are summarized in Table 4, along with a comparison with the actual values. The absolute error (|experimental value – actual value|) is presented instead of the relative error.

The accuracy in the estimated location and length is acceptable in this clean laboratory experiment. However, in field and long pipelines, where the wave speed and impedance are not uniform and hard to estimate accurately, much more error can be expected. In addition to the shape and rise time of the wave front, sampling rate may also affect the accuracy, especially for the determination of the length of the deterioration.

CONCLUSIONS

A transient-based distributed deterioration detection method has been proposed. The transient response due to a deteriorated section with an impedance change has been analyzed by the method of characteristics. Two detection strategies have been adopted to cater for different equipment configurations. A theoretical square-shaped disturbance was found to appear within the first plateau of the water hammer trace due to reflection and transmission at the two boundaries of the distributed deterioration. The current study has shown that, in principle, the location, length and impedance of the deteriorated section can be estimated from the size of the measured deterioration-induced disturbance.

The formula used to estimate the impedance of the deterioration is simple, as given in Eq. (15). It is independent of the steady-state head and flow rate, but rather only related to the impedance of the original pipeline and the magnitude ratio of the reflected disturbance to the incident wave. The estimated impedance is accurate when the duration of the initial wave front is less than the time for the wave traveling twice the length of the deterioration. When the initial wave front has a longer duration, the results will be compromised.

The proposed distributed deterioration detection method was applied to the interpretation of experimental data measured from a pipeline with a section of decreased

uniform wall thickness. The impedance of this deteriorated section was successfully estimated from three of the repeated experimental pressure traces. The wall thickness and wave speed were obtained, assuming that the uniform wall thickness change was the sole source of the impedance alternation. The location and the length of the deterioration were determined using time-domain reflectometry (TDR). The accuracy of these results was acceptable, indicating that the proposed technique is valid under controlled laboratory conditions.

ACKNOWLEDGEMENTS

The research presented in this paper has been supported by the Australia Research Council through the Discovery Project Grant DP1095270. The first author thanks the Chinese Scholarship Council and the University of Adelaide for providing a joint postgraduate scholarship.

REFERENCES

Arbon, N. S., Lambert, M. F., Simpson, A. R., and Stephens, M. L. (2007). "Field test investigations into distributed fault modeling in water distribution systems using transient testing." *World Environmental and Water Resources Congress 2007*, Tampa, Florida, United States.

Colombo, A. F., Lee, P., and Karney, B. W. (2009). "A selective literature review of transient-based leak detection methods." *Journal of Hydro-environment Research*, 2(4), 212-227.

Kim, Y. (2008). "Advanced Numerical and Experimental Transient Modelling of Water and Gas Pipeline Flows Incorporating Distributed and Local Effects," PhD thesis, University of Adelaide, Adelaide.

Kim, Y., Simpson, A. R., and Lambert, M. F. (2007). "The effect of orifices and blockages on unsteady pipe flows." *World Environmental and Water Resources Congress 2007*, Tampa, Florida, United States.

Lee, P. J., Vítkovský, J. P., Lambert, M. F., Simpson, A. R., and Liggett, J. A. (2005). "Leak location using the pattern of the frequency response diagram in pipelines: a numerical study." *Journal of Sound and Vibration*, 284(3-5), 1051–1073.

Lee, P. J., Lambert, M. F., Simpson, A. R., Vítkovský, J. P., and Liggett, J. A. (2006). "Experimental verification of the frequency response method for pipeline leak detection." *Journal of Hydraulic Research, IAHR*, 44(5), 693–707.

Lee, P. J., Vítkovský, J. P., Lambert, M. F., Simpson, A. R., and Liggett, J. A. (2007a). "Leak location in pipelines using the impulse response function." *Journal of Hydraulic Research, IAHR*, 45(5), 643-652.

Lee, P. J., Lambert, M. F., Simpson, A. R., Vítkovský, J. P., and Misiunas, D. (2007b). "Leak location in single pipelines using transient reflections." *Australian Journal of Water Resources*, 11(1), 53-65.

Lee, P. J., Vítkovský, J. P., Lambert, M. F., Simpson, A. R., and Liggett, J. A. (2008). "Discrete blockage detection in pipelines using the frequency response diagram: numerical study." *Journal of Hydraulic Engineering, ASCE*, 134(5), 658-663.

Nawrocki, J., Raczyk-Stanisawiak, U., Swietlik, J., Olejnik, A., and Sroka, M. J. (2010). "Corrosion in a distribution system: Steady water and its composition." *Water Research*, 44(6), 1863-1872.

Rajani, B., and Kleiner, Y. (2001). "Comprehensive review of structural deterioration of water mains: physically based models." *Urban Water*, 3(3), 151-164.

Sarin, P., Snoeyink, V. L., Bebee, J., Kriven, W. M., and Clement, J. A. (2001). "Physico-chemical characteristics of corrosion scales in old iron pipes." *Water Research*, 35(12), 2961-2969.

Stephens, M. L., Simpson, A. R., and Lambert, M. F. (2008). "Internal wall condition assessment for water pipelines using inverse transient analysis." *10th Annual Symposium on Water Distribution Systems Analysis, ASCE*, Kruger National Park, South Africa, 911-921.

Tran, D. H., Perera, B. J. C., and Ng, A. W. M. (2010). "Hydraulic deterioration models for storm-water drainage pipes: Ordered probit versus probabilistic neural network." *Journal of Computing in Civil Engineering*, 24(2), 140-150.

Vítkovský, J. P., Lee, P. J., Spethens, M. L., Lambert, M. F., Simpson, A. R., and Liggett, J. A. (2003). "Leak and blockage detection in pipelines via an impulse response method." *Pumps, Electromechanical Devices and Systems Applied to Urban Water Management*, Valencia, Spain, 423–430.

Vreeburg, I. J. H. G., and Boxall, D. J. B. (2007). "Discolouration in potable water distribution systems: A review." *Water Research*, 41(3), 519-529.

Wang, X. J., Lambert, M. F., Simpson, A. R., Liggett, J. A., and Vítkovský, J. P. (2002). "Leak detection in pipelines using the damping of fluid transients." *Journal of Hydraulic Engineering, ASCE*, 128(7), 697-711.

Wylie, E. B. (1983). "The microcomputer and pipeline transients." *Journal of Hydraulic Engineering, ASCE*, 109(12), 1723-1739.

Wylie, E. B., and Streeter, V. L. (1993). *Fluid Transients in Systems*, Prentice Hall Inc., Englewood Cliffs, New Jersey, USA.

Zamanzadeh, M., Kirkwood, G. C., Scheinman, S., and Bayer, G. T. (2007). "Corrosion sensors for detecting graphitization of cast iron in water mains." *Corrosion 2007*, Nashville, TN, United States, 073801-073809.

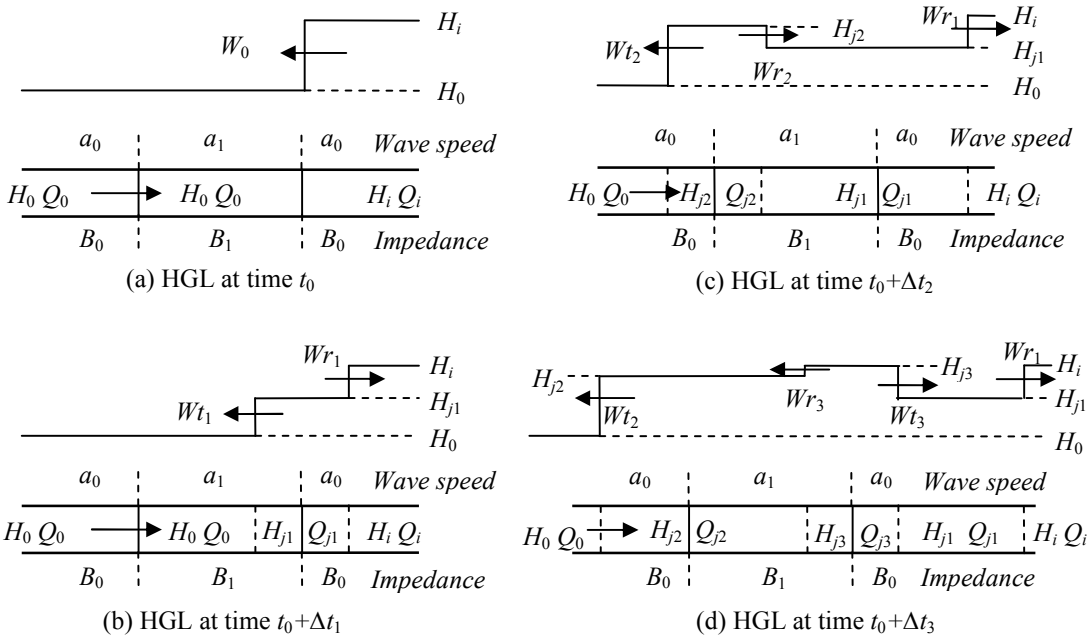

Figure 1 Illustration for a wave propagating through a deteriorated section (designated with length L_1, impedance B_1 and wave speed a_1).

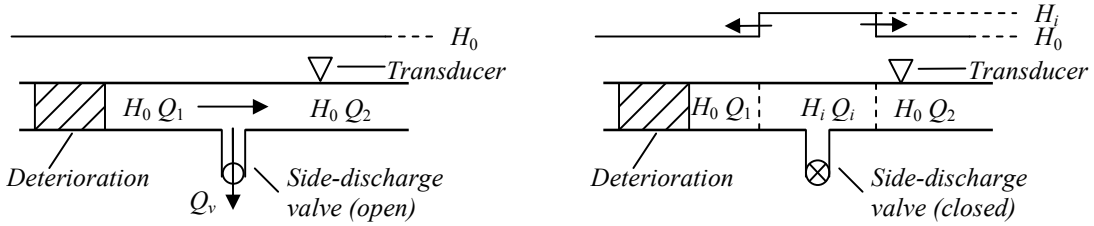

(a) HGL at time t_0 (b) HGL at time $t_0+\Delta t_1$

Figure 2 Distributed deterioration detection at an interior location within the pipeline.

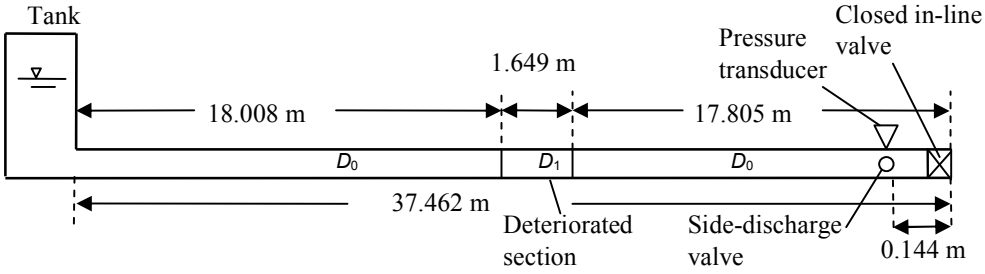

Figure 3 The experimental pipeline system layout.

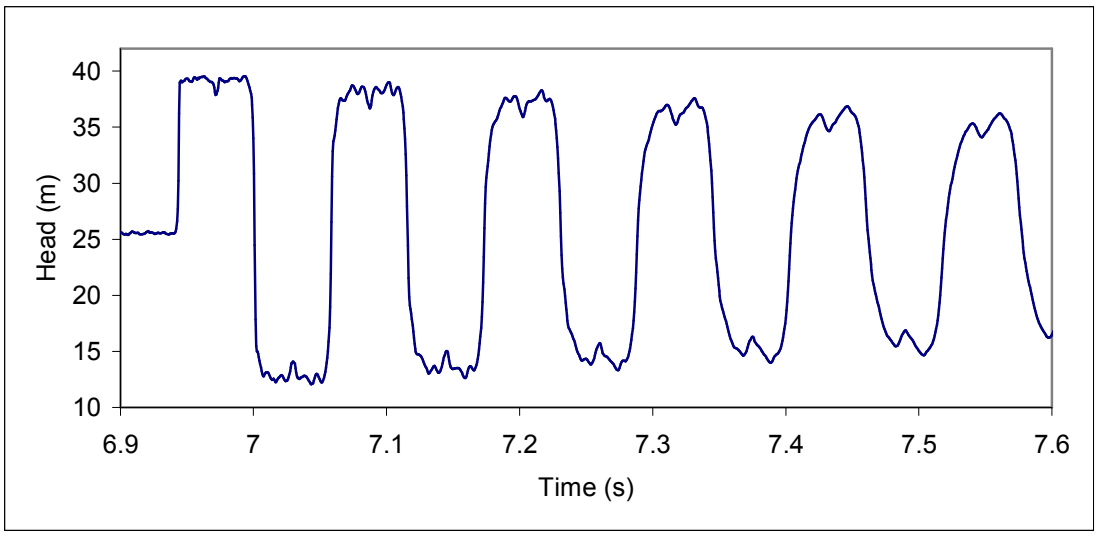

Figure 4 The experimental pressure trace of Test 1.

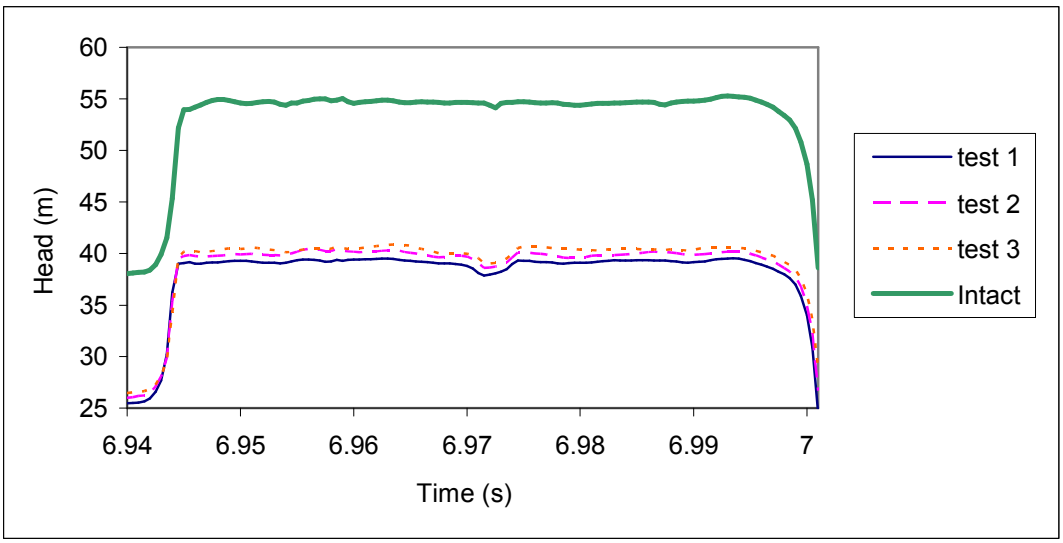

Figure 5 The first plateau of experimental head response traces. Three experiments (Tests 1 to 3) on a pipeline with a section of thinner wall thickness, compared to one experiment on an intact pipeline.

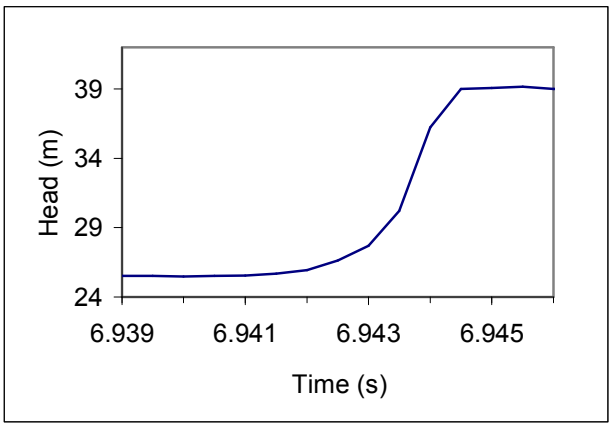

Figure 6 An enlarged view of the wave front in Test 1.

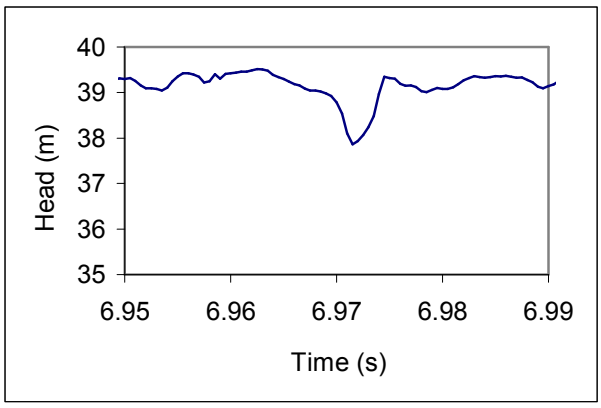

Figure 7 An enlarged view of the pressure perturbation in the first plateau of the pressure trace measured in Test 1.

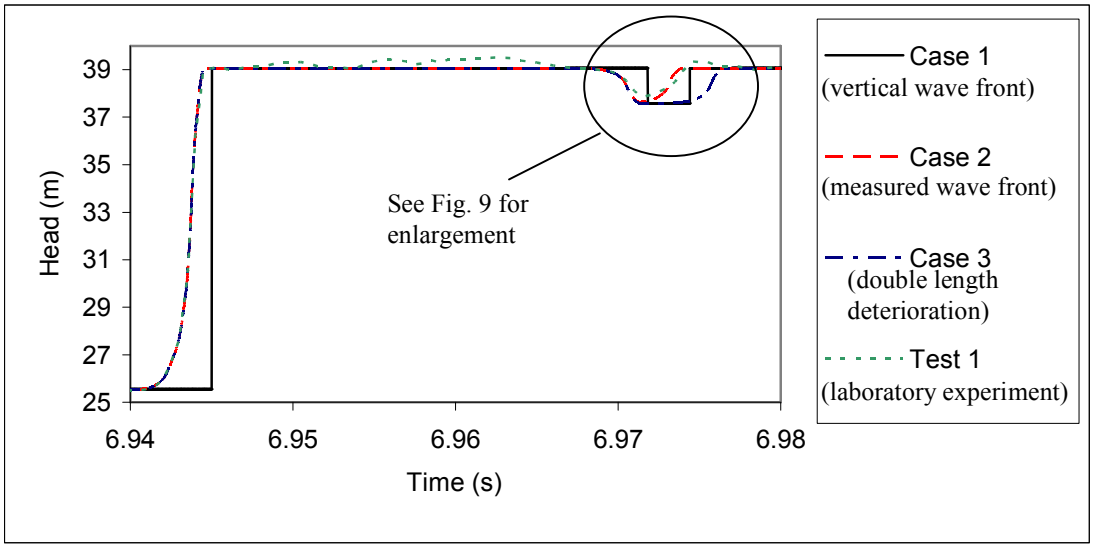

Figure 8 The pressure response traces obtained from numerical simulations. 'Case 1': using the experimental pipeline configuration and a vertical wave front; 'Case 2': using the experimental pipeline configuration and the measured wave front; 'Case 3': using the measured wave front, and the modified pipeline configuration, in which the length of the deterioration is doubled; 'Test 1': the experimental pressure trace from Test 1.

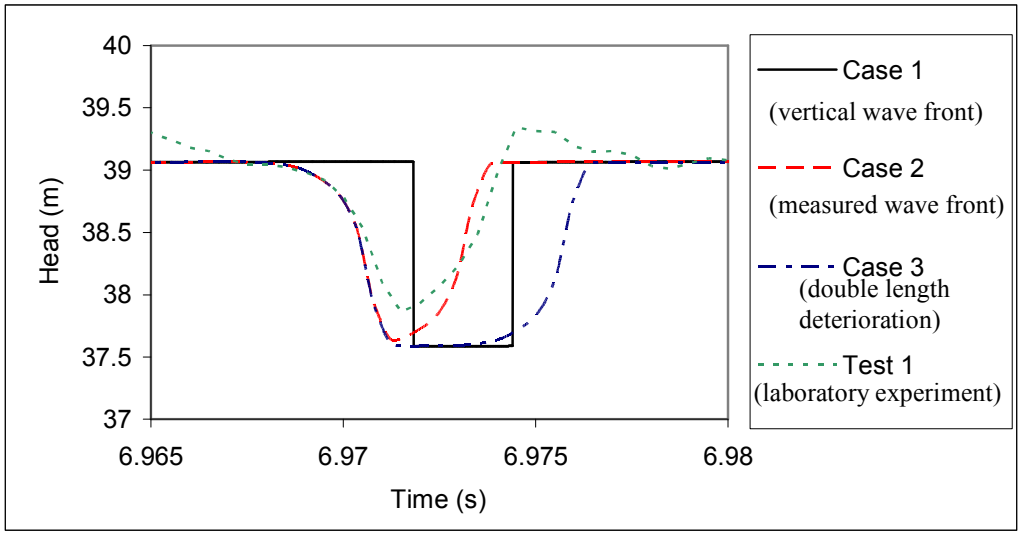

Figure 9 The deterioration-induced pressure perturbations obtained from numerical simulations (enlargement of Figure 8). 'Case 1': using the experimental pipeline configuration and a vertical wave front; 'Case 2': using the experimental pipeline configuration and the measured wave front; 'Case 3': using the measured wave front, and the modified pipeline configuration, in which the length of the deterioration is doubled; 'Test 1': the experimental pressure trace from Test 1.

Table 1. The impedance B_1, wave speed a_1 and wall thickness e_1 of the deteriorated section: 'Analytical values' are theoretical results analytically calculated for the actual wall thickness of the deteriorated section e_1 = 1.22 mm; 'Test 1' to 'Test 3' are experimental results estimated from the pressure traces measured in laboratory experiments.

Data source	Impedance B_1 (s/m^2)	Relative error*	Wave speed a_1 (m/s)	Relative error*	Wall thickness e_1 (mm)	Relative error*
Analytical values	3.151×10^5	N/A	1282	N/A	1.22	N/A
Test 1	3.217×10^5	2.1 %	1292	0.8 %	1.29	5.7 %
Test 2	3.234×10^5	2.6 %	1295	1.0 %	1.31	7.4 %
Test 3	3.217×10^5	2.1 %	1292	0.8 %	1.29	5.7 %

* Relative error = |(value estimated from tests – analytical value)/ analytical value|$\times$100%

Table 2. The difference in the impedance, wave speed and wall thickness between the deterioration and the original pipeline: 'Analytical values' are theoretical results analytically calculated for the actual wall thickness of the deteriorated section e_1 = 1.22 mm; 'Test 1' to 'Test 3' are experimental results estimated from the pressure traces measured in laboratory experiments.

Data source	Impedance difference $\Delta B = B_1 - B_0$ (s/m^2)	Relative error*	Wave speed difference $\Delta a = a_1 - a_0$ (m/s)	Relative error*	Wall thickness difference $\Delta e = e_1 - e_0$ (mm)	Relative error*
Analytical values	–36, 490	N/A	–46	N/A	–0.41	N/A
Test 1	–29, 900	18.1 %	–36	21.7 %	–0.34	17.1 %
Test 2	–28, 200	22.7 %	–33	28.3 %	–0.32	22.0 %
Test 3	–29, 900	18.1 %	–36	21.7 %	–0.34	17.1 %

* Relative error = |(value estimated from tests – analytical value)/ analytical value $| \times 100\%$

Table 3. The magnitude of the reflected disturbance and the estimated impedance difference between the deterioration and the original pipeline: 'Analytical values' are theoretical results calculated for $B_1 = 3.151\times10^5$ s/m^2; 'Case 1' to 'Case 3' are results estimated from the numerical pressure traces.

Data source	Magnitude of disturbance ΔH (m)	Relative deviation* (m)	Impedance difference ΔB (s/m^2)	Relative deviation*
Analytical values	–1.48	N/A	–36, 490	N/A
Case 1 (vertical wave front)	–1.48	0.0 %	–36, 490	0.0 %
Case 2 (measured wave front)	–1.44	2.7 %	–35, 580	2.5 %
Case 3 (double length deterioration)	–1.48	0.0 %	–36, 490	0.0 %

*Relative deviation = |(value estimated from numerical simulations – analytical value)/ analytical value | $\times$100%

Table 4. The location and length of the deteriorated section: 'Actual value' is measured from the experimental pipeline; 'Experimental result' is obtained from the proposed technique using the experimental pressure trace.

Property	Actual value	Experimental result	Absolute error*
Location L_0 (m)	17.805	17.60	0.205
Length L_1 (m)	1.649	2.56	0.911

*Absolute error = |experimental result – actual value|